Saturation of multiplexed volume Bragg grating recording

Sergiy Kaim,[1] Sergiy Mokhov,[1] Ivan Divliansky,[1] Vadim Smirnov,[2] Julien Lumeau,[3] Boris Y. Zeldovich,[1,*] and Leonid B. Glebov[1]

[1]*CREOL, The College of Optics and Photonics, University of Central Florida, Orlando, Florida 32816, USA*
[2]*OptiGrate Corp, 562 South Econ Circle, Oviedo, Florida 32765-4311, USA*
[3]*Aix-Marseille Université, CNRS, Centrale Marseille, Institut Fresnel, UMR 7249, 13013 Marseille, France*
**Corresponding author: boris@creol.ucf.edu*

Received September 11, 2014; accepted October 15, 2014;
posted November 4, 2014 (Doc. ID 222938); published December 4, 2014

Recording of volume Bragg gratings (VBGs) in photo-thermo-refractive glass is limited to a maximum refractive index change about 0.002. We discuss various saturation curves and their influence on the amplitudes of recorded gratings. Special attention is given to multiplexed VBGs aimed at recording several gratings in the same volume. The best shape of the saturation curve for production of the strongest gratings is the threshold-type curve. Two-photon absorption as a mechanism of recording also allows increasing the strength of multiplexed VBGs. © 2014 Optical Society of America

OCIS codes: (050.7330) Volume gratings; (090.4220) Multiplex holography.
http://dx.doi.org/10.1364/JOSAA.32.000022

1. INTRODUCTION

Volume Bragg gratings (VBGs) [1,2] recorded in photo-thermo-refractive glass (PTRG) constitute a new set of optical elements. They are used for spectral combining of high-power laser beams [3–5], for stretching and compression of ultrashort pulses [6,7], for mode stabilization of diode lasers [8], for passive coherent beam combining [9], and for narrowband filtering in different fields of spectroscopy [10,11]. Many of these elements are multiplexed VBGs, that is, they contain several gratings with different spatial frequencies. Amplitudes of recorded gratings, both single and multiplexed ones, namely spatial Fourier components of recorded $\delta n(\mathbf{r})$, are limited due to the fact of saturation of refractive index change by the value $\Delta n_{\max}$. In the case of PTRG the value of $|\Delta n_{\max}|$ in the best condition of recording and thermal development of VGBs is about $|\Delta n_{\max}| \approx 0.002$.

Recording several volume holograms in the same volume has been studied theoretically and experimentally in [12–14] and numerous other works, with the purpose of data storage. Those studies were aimed to maximize the number of recorded holograms. The requirements for diffraction efficiency of each individual grating were not very stringent: the diffracted wave had to be detectable at the level of rather weak noise. Most of those data-storage works were discussing and implementing multiplexed recording in electro-optic photorefractive crystals. Those crystals do not have strong response to the pedestal of recording beam intensity [15]; therefore only small spatial period (spatial AC) components of the illumination at recording were accounted for. As a result, the mean square average amplitude of spatial AC modulation grows as $\sqrt{N}$, where N is the number of gratings with independent periods and independent phases [13].

The main application of PTRG-based VBGs, both single and multiplexed ones, is handling high-power beams, be they inside the laser cavity or outside it. Therefore the achievement of large diffraction efficiency via generating a strong spatial Fourier-component of refractive index modulation is of the essence. Exposure of the medium via single-photon absorption of interference patterns of a pair of coherent waves with identical intensities and identical polarization is assumed to be

$$U(\mathbf{r}) = 0.5U_1 \cdot |\exp(i\mathbf{kr}) + \exp[i(\mathbf{k}+\mathbf{q}_1)\mathbf{r} + i\varphi_1]|^2 = U_1[1+\cos(\mathbf{q}_1\mathbf{r}+\varphi_1)].$$

The main feature of a PTRG-VBG is that the pedestal part (spatially uniform), U_1, of the exposure counts with the same coefficient as the grating part (spatially periodic), $U_1\cos(\mathbf{q}_1\mathbf{r}+\varphi_1)$. For a large degree of multiplexing, $N \gtrsim 4$, it is the saturation of the recording response by the sum of the pedestals, $\sum_j U_j \sim U_1 N$, that is the crucial factor. Meanwhile, individual gratings, $U_j\cos(\mathbf{q}_j\mathbf{r}+\varphi_j)$, have random phases, and their rms amplitude grows as $U_1\sqrt{N}$.

In this work we study theoretically the influence of saturation on recorded VBGs taking into account of the following factors:

(1) Normalized shape $\rho(U)$ of the saturation curve, that is, dependence of refractive index change upon total exposure $U(\mathbf{r})$: $\delta n(\mathbf{r}) = \Delta n_{\max}\cdot\rho(U(\mathbf{r}))$.
(2) Number N of individual gratings intended to be recorded.
(3) Spatially average exposure $\langle U\rangle \approx U_1 N$ due to pedestal.

2. SHAPES OF SATURATION CURVE $\rho(U(r)) = \delta n(r)/\Delta n_{\max}$

As presented below, seven different shapes $\rho(U)$ chosen for our study are normalized in such a way that $\rho(U\to\infty) = 1$. Besides that, the first five curves under consideration have

the property $\rho(U \to 0) = 1 \cdot U$. The latter condition just means the choice of units of exposure. Here are the seven different shapes that we have considered:

$$\rho_{\tanh}(U) = \tanh(U), \tag{1}$$

$$\rho_{\arctan}(U) = (2/\pi)\arctan(\pi U/2), \tag{2}$$

$$\rho_{\text{power}}(U) = U/(1+U), \tag{3}$$

$$\rho_{\exp}(U) = 1 - \exp(-U), \tag{4}$$

$$\rho_{\text{line}\,45}(U) = \begin{cases} U & \text{at } 0 < U < 1 \\ 1 & \text{at } U > 1 \end{cases}, \tag{5}$$

$$\rho_{\text{line}\,60}(U) = \begin{cases} 0 & \text{at } 0 < U < 0.5 \\ 2(U-0.5) & \text{at } 0.5 < U < 1 \\ 1 & \text{at } U > 1 \end{cases}, \tag{6}$$

$$\rho_{\text{heaviside}}(U) = \begin{cases} 0 & \text{at } 0 < U < 0.5 \\ 1 & \text{at } U > 0.5 \end{cases}. \tag{7}$$

By the saturation curve $\rho(U)$ we denote the function $\rho(U)$ in the relationship that we assume in our model:

$$\delta n(\mathbf{r}) = \Delta n_{\max} \cdot \rho(U(\mathbf{r})). \tag{8}$$

Figure 1 shows the graphs of those seven functions; we put them into two different pictures to reduce the clutter.

It should be emphasized that there is no experimental evidence that the recording in PTRG satisfies any particular saturation law. Some theoretical models of PTRG recording and development point to a power law, Eq. (3), as a rather plausible variant [2]. However, the purpose of this modeling work is to make predictions following from all seven hypotheses, Eqs. (1)–(7), with the aim of subsequent comparison with future detailed experiments.

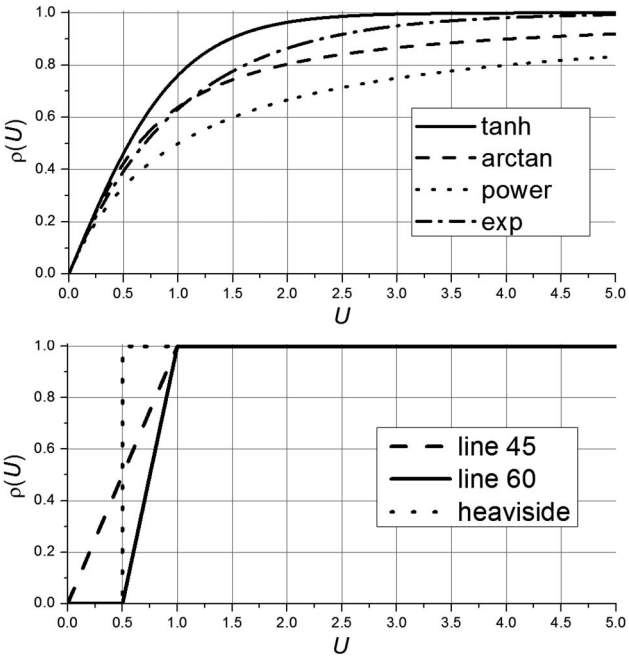

Fig. 1. Shapes of seven saturation curves under consideration.

3. MODELS OF EXPOSURE

We assume that an individual grating is recorded via the interference pattern of two coherent waves. Intensity in such an interference pattern is

$$U_j(1 + \cos(\mathbf{q}_j\mathbf{r} + \varphi_j)). \tag{9}$$

For single-photon absorption, the exposure by N sequential interference patterns is

$$U(\mathbf{r}) = \sum_{j=1}^{N} U_j[1 + \cos(\mathbf{q}_j\mathbf{r} + \varphi_j)]. \tag{10}$$

For definiteness we consider all N intensities U_j to be the same: $U_j = U_1$. Meanwhile the wave vectors $\mathbf{q}_j$ and phases φ_j are considered to be statistically independent random quantities in our model.

For two-photon absorption of the recording pattern of interference we take

$$\begin{aligned} &U_j^2[1 + \cos(\mathbf{q}_j\mathbf{r} + \varphi_j)]^2 \\ &\equiv U_j^2\left[1 + 2\cos(\mathbf{q}_j\mathbf{r} + \varphi_j) + \frac{1}{2} + \frac{1}{2}\cos(2\mathbf{q}_j\mathbf{r} + 2\varphi_j)\right] \\ &\equiv \frac{3}{2}U_j^2\left[1 + \frac{4}{3}\cos(\mathbf{q}_j\mathbf{r} + \varphi_j) + \frac{1}{3}\cos(2\mathbf{q}_j\mathbf{r} + 2\varphi_j)\right]. \end{aligned} \tag{11}$$

Note that relative modulation term at the "right" spatial frequency has increased by a factor of 4/3. Besides that,

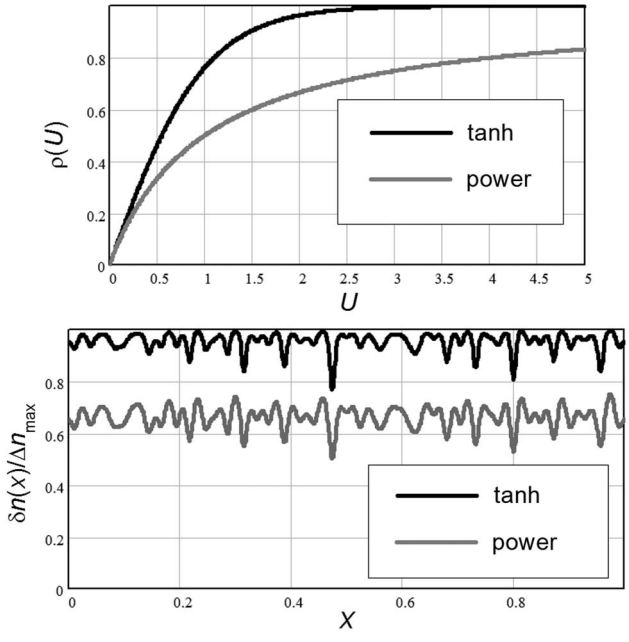

Fig. 2. (a) Two saturation curves, Eqs. (1) and (3); (b) spatial profile of refractive index change of recording 16 multiplexed gratings.

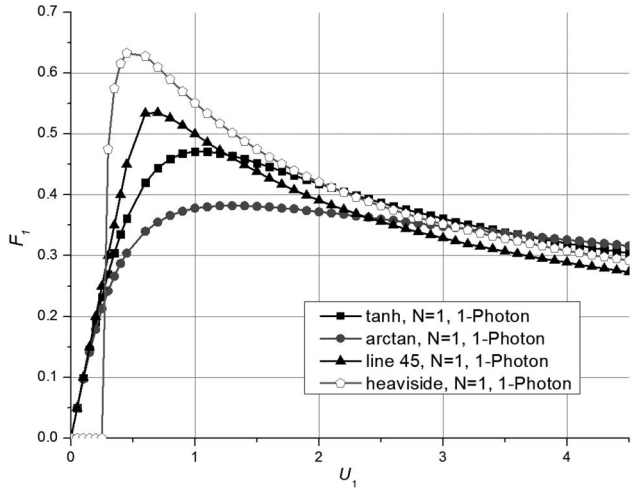

Fig. 3. Dependence of Fourier amplitude F_j of a single recorded grating on average exposure U_1 for different laws of saturation in the case of one-photon absorption.

the second spatial harmonic appears in $U(\mathbf{r})$ for two-photon recording.

Figure 2 illustrates Eqs. (1) and (3) and the spatial profile of the refractive index change for the case of $N = 16$ independently recorded interference grating patterns with particular arbitrary values of $\mathbf{q}_j$ and φ_j. Spatially average exposure was chosen as $U_1 N = 2.25$.

4. FOURIER COMPONENT TO BE CALCULATED

By the Fourier component of a VBG we denote the quantity

$$F_j = \frac{2}{V} \iiint \cos(\mathbf{q}_j \mathbf{r} + \varphi_j) \rho(U(\mathbf{r})) \mathrm{d}^3\mathbf{r}. \tag{12}$$

Here the trivial factor $\Delta n_{\max}$ is omitted. The normalization coefficient $2/V$, with V being the integration volume, is chosen in such a way that for the first five curves of saturation $\rho_\alpha(U)$ the value of F_j is equal to U_j at $NU_1 \ll 1$. In actual calculations we used a one-dimensional integral over the interval length L, with normalization coefficient $2/L$:

$$F_j = \frac{2}{L} \int_0^L \cos(q_j x + \varphi_j) \rho(U(x)) \mathrm{d}x. \tag{13}$$

The values of $q_j L$ were around 100 rad and more; q_j were chosen to be mutually noncommensurate; and phases φ_j were random within the interval $(0, 2\pi)$. We successfully checked that if some particular component $U_k[1 + \cos(q_k x + \varphi_k)]$ was absent during recording, then the Fourier-component F_k calculated by Eq. (13) was much smaller than those F_j, whose $U_j[1 + \cos(q_j x + \varphi_j)]$ were actually present at recording.

5. RESULTS FOR RECORDING OF SINGLE VBG

Our first step was to find the dependence of the Fourier component of $\delta n(\mathbf{r})$ for recording of a single grating: $N = 1$, on the value of exposure $NU_1 \equiv U_1$. Figure 3 shows the dependence of F_1 on U_1 for four out of the seven studied curves of saturation: $\tanh(U)$, $(2/\pi)\arctan(\pi U/2)$, straight linear between $(U = 0, \rho = 0)$ and $(U = 1, \rho = 1)$, and step-function from 0 to 1 at $U = 0.5$. All seven studied laws of saturation have demonstrated a peak of F_1 around $U_1 \sim 1$ and a decrease of F_1 for large U_1. To eliminate clutter on the graph, we depicted only four curves corresponding to Eqs. (1), (2), (5), and (7). The peak values of the F_1 peak and the corresponding exposure U_1 delivering that F_1 peak for all seven saturation laws are presented in the first pair of lines of Table 1.

The qualitative conclusion is that sharper $\rho(U)$ curves yield larger values of $F_{1,\mathrm{peak}}$. However, the difference between the largest $F_{1,\mathrm{peak}}$ for $\rho_{\mathrm{heaviside}}(U)$ and the smallest $F_{1,\mathrm{peak}}$ for power law saturation constitutes only a factor around 1.85. The curves in Fig. 3 and the data in Table 1 were produced for a single-photon absorption model of recording. Corresponding data for the two-photon absorption model of recording are presented in Fig. 4 and Table 2.

6. MULTIPLEXED VBG WITH $N = 4,8,16,32$, AND 64 GRATINGS

Figure 5 shows the average Fourier component $\langle F_j \rangle$ for $j = 1, 2, 3, 4$ at single-photon recording of $N = 4$ independent gratings, while Fig. 6 shows the same results for two-photon absorption. Figure 7 shows results for one-photon absorption for $N = 32$ independent gratings. Again, as on Fig. 3, we tried not

Table 1. Peak Fourier Amplitudes for All Seven Functions for $N = 1,4,8,16,32$, and 64 Gratings in the Case of One-Photon Absorption

N		Tanh	Arctan	Power	Exp	Line 45	Line 60	Heaviside
1	F_1 peak	0.472	0.382	0.343	0.438	0.536	0.625	0.637
	$N \cdot U_1$ for peak value	1.05	1.3	2.45	1.55	0.65	0.8	0.5
4	F_1 peak	0.113	0.083	0.068	0.097	0.160	0.267	0.298
	$N \cdot U_1$ for peak value	0.833	0.752	1.249	1.129	0.752	0.752	0.502
8	F_1 peak	0.056	0.041	0.033	0.047	0.086	0.158	0.199
	$N \cdot U_1$ for peak value	0.833	0.680	1.129	1.129	0.752	0.752	0.502
16	F_1 peak	0.028	0.020	0.016	0.023	0.046	0.090	0.142
	$N \cdot U_1$ for peak value	0.752	0.020	1.020	1.020	0.752	0.833	0.501
32	F_1 peak	0.014	0.01	0.01	0.012	0.025	0.049	0.101
	$N \cdot U_1$ for peak value	0.752	0.614	1.249	1.020	0.833	0.833	0.502
64	F_1 peak	0.007	0.006	0.004	0.007	0.013	0.026	0.072
	$N \cdot U_1$ for peak value	0.462	0.566	0.502	0.752	0.833	0.833	0.502

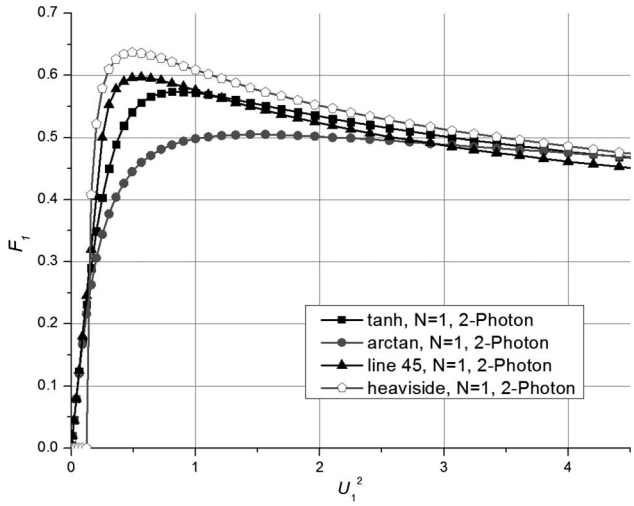

Fig. 4. Same graph as Fig. 3 but for the case of two-photon absorption.

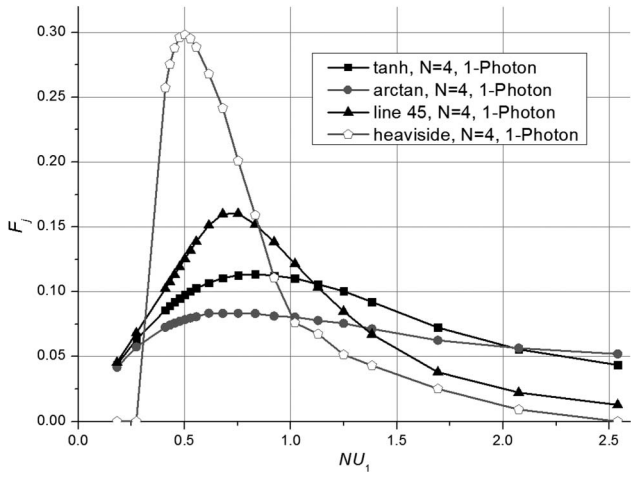

Fig. 5. Dependence of Fourier amplitude F_j of $N = 4$ gratings on average exposure NU_1 for various laws of saturation in the case of one-photon absorption.

to overburden the graph by keeping the curves for four laws of saturation only. The argument on the horizontal axis is the spatially averaged exposure $U_{\text{av}} = NU_1$. Table 1 gives the peak values of average Fourier component F_j (peak) and the spatially average exposure $NU_j \equiv NU_1$ delivering that peak. Figure 8 and Table 2 provide similar information for the model of two-photon absorption.

7. DEPENDENCE OF PEAK FOURIER AMPLITUDE F_j ON MULTIPLEXITY N: ANALYTIC CALCULATIONS AND NUMERICAL MODELING

Analytic calculations for a large number of individually recorded gratings may be done via the decomposition $U(\mathbf{r}) = NU_1 + \sum_{j=1}^{N} U_1 \cos(\mathbf{q}_j\mathbf{r} + \varphi_j)$ for the single-photon case, so that

$$n(x) = \Delta n_{\max}\left[\rho(\xi) + \frac{\partial\rho}{\partial\xi}U_1 \cos(q_j x + \varphi_j)\right], \qquad \xi = NU_1,$$

$$F_j = \frac{\partial\rho}{\partial\xi}U_j \equiv \frac{1}{N}\xi\frac{\partial\rho}{\partial\xi}. \tag{14}$$

The values of the maxima of functions $\xi\partial\rho/\partial\xi$ are $[\xi\partial\rho_{\text{tanh}}/\partial\xi]_{\max} = 0.448$, $[\xi\partial\rho_{\text{arctan}}/\partial\xi]_{\max} = 1/\pi = 0.38$, $[\xi\partial\rho_{\text{power}}/\partial\xi]_{\max} = 1/4 = 0.25$, $[\xi\partial\rho_{\exp}/\partial\xi]_{\max} = e^{-1} = 0.368$, $[\xi\partial\rho_{\text{line }45}/\partial\xi]_{\max} = 1$, and $[\xi\partial\rho_{\text{line }60}/\partial\xi]_{\max} = 2$ at $\xi_{\text{tanh}} = 0.776$, $\xi_{\text{arctan}} = 2/\pi = 0.637$, $\xi_{\text{power}} = 1$, $\xi_{\exp} = 1$, $\xi_{\text{line }45} = 1$, and $\xi_{\text{line }60} = 1$, respectively.

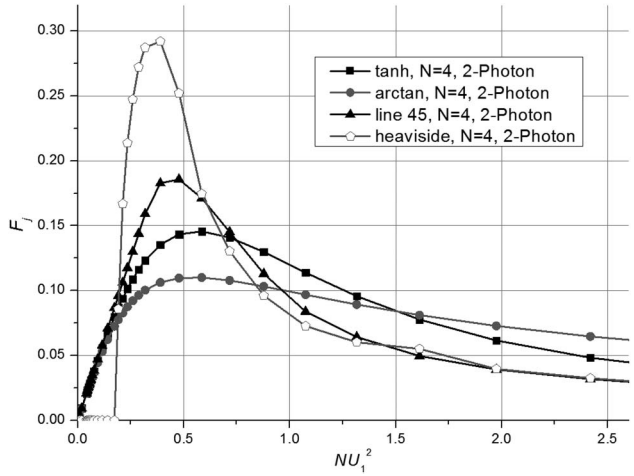

Fig. 6. Same graph as on Fig. 5, but for the case of two-photon absorption.

Table 2. Peak Fourier Amplitudes for All Seven Functions for N = 1,4,8,16,32, and 64 Gratings in the Case of Two-Photon Absorption

N		Tanh	Arctan	Power	Exp	Line 45	Line 60	Heaviside
1	F_1 peak	0.574	0.505	0.476	0.556	0.597	0.633	0.637
	$N \cdot U_1$ for peak value	0.81	1.44	2.89	1.21	0.563	0.723	0.49
4	F_1 peak	0.145	0.110	0.092	0.127	0.186	0.272	0.292
	$N \cdot U_1$ for peak value	0.585	0.585	0.878	0.717	0.478	0.478	0.390
8	F_1 peak	0.074	0.054	0.044	0.062	0.104	0.173	0.198
	$N \cdot U_1$ for peak value	0.537	0.476	0.658	0.658	0.476	0.537	0.358
16	F_1 peak	0.037	0.028	0.021	0.030	0.056	0.104	0.139
	$N \cdot U_1$ for peak value	0.514	0.343	0.711	0.437	0.514	0.514	0.343
32	F_1 peak	0.018	0.013	0.011	0.015	0.030	0.060	0.099
	$N \cdot U_1$ for peak value	0.555	0.453	0.680	0.680	0.555	0.555	0.328
64	F_1 peak	0.009	0.006	0.005	0.008	0.016	0.033	0.069
	$N \cdot U_1$ for peak value	0.510	0.434	0.706	0.706	0.553	0.553	0.327

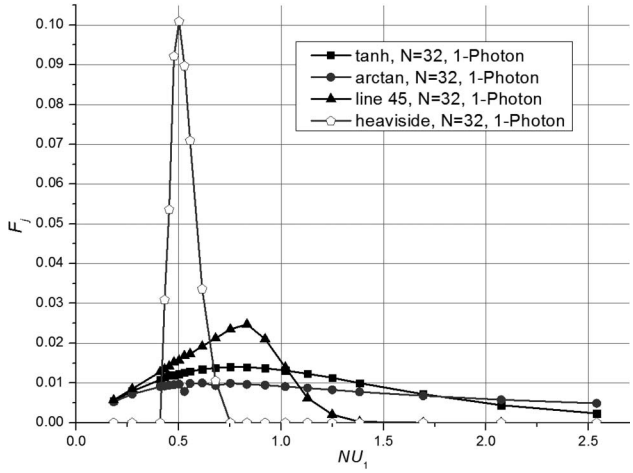

Fig. 7. Dependence of Fourier amplitude F_j of $N = 32$ gratings on average exposure NU_1 for different laws of saturation in the case of one-photon absorption.

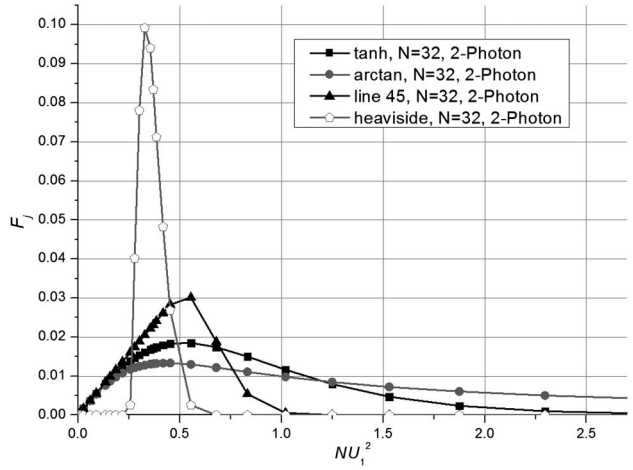

Fig. 8. Same graph as on Fig. 7, but for the case of two-photon absorption.

The results of numerical modeling yield reasonable agreement with Eq. (14) at least for $N \geq 4$.

Special attention should be paid to the case of the Heaviside function, $\rho_{\text{heaviside}}(\xi)$, at $\xi = 0.5$. The optimal value of $NU_1 = \xi_{\text{opt}}$ is evidently $\xi_{\text{opt,heaviside}} = 0.5$, so that $U_{1\ \text{opt,heaviside}} = 0.5/N$.

After that one should consider $u(x) \approx 0.5 + r + m(x)$. Here $m(x) = U_1 \cos(q_1 x)$, and r is a random quantity, which is the result of adding all spatially oscillating parts of all the remaining sinusoidal profiles of the recording; that is, the other recorded gratings. The probability distribution $W(r)dr$, due to the central limit theorem, is well approximated by the Gaussian $W(r)dr \approx (2\pi\sigma^2)^{-0.5} \exp(-r^2/2\sigma^2)\, dr$, where $\sigma^2 \approx 0.5\, NU_j^2$. Taking into account the optimum $U_j = 0.5/N$, the square of the standard deviation for r becomes $\sigma^2 \approx 1/(8\, N)$. This means that the value of $\rho_{\text{st}}(0.5 + r + m(x))$, averaged over fluctuations of r, approximately equals $W(0)m(x) = m(x)\sqrt{4\, N/\pi}$. Further spatial averaging of $\cos^2(q_1 x)$ yields a factor of 0.5, and taking into account $U_1 \approx 0.5/N$ one gets the optimum multiplexed grating for the Heaviside response of a multiplexed VBG $F_j \approx 1/\sqrt{\pi N}$.

This result is also in reasonable agreement with numerical modelling at $N \gg 1$.

In the case of two-photon recording the value of optimum ξ for different $\rho(U)$ curves should be equalized to $N \cdot (3U_1^2/2)$ and

$$F_j = 2U_1^2\left(\xi\frac{d\rho}{d\xi}\right)_{\text{opt}} = \frac{4}{3}\left(\xi_{\text{opt}}\frac{d\rho}{d\xi}\right)\frac{1}{N}, \qquad U_1^2 = \frac{2\xi_{\text{opt}}}{3\, N}. \quad (15)$$

Again, numerical modeling at $N \gg 1$ is in reasonable agreement with this extra factor 4/3 for two-photon recording.

Quite interesting is the problem of cross-modulation gratings. Namely, if the recording profile contains, among others, the terms $U_j(1 + \cos(q_j x + \varphi_j))$ and $U_k(1 + \cos(q_k x + \varphi_k))$, then a grating

$$\delta n(x) = \Delta n_{\max} \cdot F_{jk} \cdot \left\{\cos\left[(q_j + q_k)x + \varphi_j + \varphi_k\right] + \cos\left[(q_j - q_k)x + \varphi_j - \varphi_k\right]\right\},$$

is recorded. Again, at $N \gtrsim 4$ analytic expansion of $\rho(U)$ around $U = NU_1$ allows us to predict

$$F_{jk} \approx \frac{1}{2\, N^2}\left[U^2\frac{d^2\rho(U)}{dU^2}\right]_{U=\langle U\rangle=NU_1}. \quad (16)$$

Thus the amplitude of "parasitic" cross-modulation gratings decreases as $1/N^2$, if the spatial average exposure $U_1 N$ is chosen to optimize the amplitudes of main gratings. Our numerical modelling with random phases φ_j and φ_k is in good agreement with analytical expression (16).

8. CONCLUSION

We have studied theoretically the recording of multiplexed VBGs with account of seven possible shapes of saturation curves. Optimum values of spatially averaged total exposure were found for each of those saturation curves and the corresponding Fourier amplitudes of individual gratings. For relatively large multiplicity, or number of gratings $N \gtrsim 4$, analytical formulae (14) through (15), derived by us, are in good correspondence with the results of numerical modeling. In particular, the best amplitude of individual Fourier components goes down as const/N, and values of that const are determined for each normalized saturation curve $\rho(U)$ on exposure U.

The qualitative conclusion is that sharper profiles of saturation curve $\rho(U)$ yield larger Fourier amplitudes at optimum exposure. Especially good would be a threshold-like profile $\rho(U)$ of the Heaviside function. A similar beneficial effect shows at sharper saturation due to two-photon recording. However, the price one should pay for this sharpness-provided advantage is the necessity of more precise adjustment of spatially averaged exposure/development.

ACKNOWLEDGMENTS

This work was supported by HEL JTO contract W911NF-10-1-0441.

REFERENCES

1. L. Glebov, "Volume holographic elements in a photo-thermo-refractive glass," J. Holography Speckle **5**, 77–84 (2009).
2. J. Lumeau and L. B. Glebov, "Effect of the refractive index change kinetics of photosensitive materials on the diffraction efficiency of reflecting Bragg gratings," Appl. Opt. **52**, 3993–3997 (2013).
3. A. Sevian, O. Andrusyak, I. Ciapurin, V. Smirnov, G. Venus, and L. Glebov, "Efficient power scaling of laser radiation by spectral beam combining," Opt. Lett. **33**, 384–386 (2008).
4. O. Andrusyak, V. Smirnov, G. Venus, V. Rotar, and L. Glebov, "Spectral combining and coherent coupling of lasers by volume Bragg gratings," IEEE J. Sel. Top. Quantum Electron. **15**, 344–353 (2009).
5. D. Ott, I. Divliansky, B. Anderson, G. Venus, and L. Glebov, "Scaling the spectral beam combining channels in a multiplexed volume Bragg grating," Opt. Express **21**, 29620–29627 (2013).
6. G. Chang, M. Rever, V. Smirnov, L. Glebov, and A. Galvanauskas, "Femtosecond Yb-fiber chirped-pulse-amplification system based on chirped-volume Bragg gratings," Opt. Lett. **34**, 2952–2954 (2009).
7. S. Kaim, S. Mokhov, B. Y. Zeldovich, and L. B. Glebov, "Stretching and compressing of short laser pulses by chirped volume Bragg gratings: analytic and numerical modeling," Opt. Eng. **53**, 051509 (2014).
8. G. B. Venus, A. Sevian, V. Smirnov, and L. B. Glebov, "High-brightness narrow-line laser diode source with volume Bragg-grating feedback," Proc. SPIE **5711**, 166–176 (2005).
9. S. Mokhov, A. Jain, C. Spiegelberg, V. Smirnov, O. Andrusyak, G. Venus, B. Zeldovich, and L. Glebov, "Multiplexed reflective volume Bragg grating for passive coherent beam combining," in *Frontiers in Optics 2010/Laser Science XXVI* (OSA, 2010), paper LWG2.
10. V. Smirnov, J. Lumeau, S. Mokhov, B. Y. Zeldovich, and L. B. Glebov, "Ultranarrow bandwidth moiré reflecting Bragg gratings recorded in photo-thermo-refractive glass," Opt. Lett. **35**, 592–594 (2010).
11. A. L. Glebov, O. Mokhun, A. Rapaport, S. Vergnole, V. Smirnov, and L. B. Glebov, "Volume Bragg gratings as ultra-narrow and multiband optical filters," Proc. SPIE **8428**, 84280C (2012).
12. L. Solymar, "Two-dimensional *N*-coupled-wave theory for volume holograms," Opt. Commun. **23**, 199–202 (1977).
13. D. Psaltis, D. Brady, and K. Wagner, "Adaptive optical networks using photorefractive crystals," Appl. Opt. **27**, 1752–1759 (1988).
14. J. R. Wullert II and Y. Lu, "Limits of the capacity and density of holographic storage," Appl. Opt. **33**, 2192–2196 (1994).
15. P. Günter and J. P. Huignard, *Photorefractive Materials and Their Applications 1: Basic Effects* (Springer, 2005), Vol. **2**.